THE JOURNAL OF Ammonia Energy

Available online at

jae.cardiffuniversitypress.org

ISSN **2752-7735**
The Journal of Ammonia Energy 03 (2025) 054–072

Cardiff University Press | Gwasg Prifysgol Caerdydd

A compact kinetic reaction mechanism for NH3/H2 flames

Alnasif A[a,b], Jójka J[c], Papp M[d], Szanthoffer AG[d,e], Kovaleva M[a], Turányi[d] T, Mashruk[a] S, Valera-Medina[a]* A, Nagy[f]* T

[a] *College of Physical Sciences and Engineering, Cardiff University, Cardiff, CF24 3AA, United Kingdom*
[b] *Engineering Technical College of Al-Najaf, Al-Furat Al-Awsat Technical University, Najaf, 31001, Iraq*
[c] *Institute of Thermal Engineering, Poznan University of Technology, 60-965 Poznan, Poland*
[d] *Institute of Chemistry, ELTE Eötvös Loránd University, Budapest, 1117, Hungary*
[e] *Hevesy György PhD School of Chemistry, ELTE Eötvös Loránd University, Budapest, 1117, Hungary*
[f] *Institute of Materials and Environmental Chemistry, HUN-REN Research Centre for Natural Sciences, Budapest, 1117, Hungary*
[*] *ValeraMedinaA1@cardiff.ac.uk, nagy.tibor@ttk.hu*

Abstract

Ammonia (NH_3) has been considered a potential fuel for energy production to achieve zero carbon emissions. However, several challenges must be addressed to ensure its widespread use and safety. The current work focuses on developing a kinetic reaction mechanism that not only accurately predicts laminar flame speeds and the emissions from NH_3 and NH_3/H_2 flames across various conditions but also ensures seamless applicability in Computational Fluid Dynamics (CFD) simulations, particularly in scenarios involving turbulent flows, such as swirl burners or complex engine chamber conditions. Using code Optima++, the rate parameters of the San Diego NH_3 mechanism (only 21 species and 64 reactions) were optimised against a large collection of laminar burning velocity data, and concentration data measured in jet-stirred reactors and burner-stabilised stagnation flame experiments to develop a compact, yet robust model for CFD simulations. Due to its small size, the mechanism lacks important chemical pathways, so the requirement for physically realistic rate coefficients had to be sacrificed in order to achieve the best possible predictivity for practical applications. The mechanism has been tested for 70/30 vol% NH_3/H_2 mixtures in CFD simulations of a general swirl burner against experimentally measured concentrations. Its predictions demonstrated good qualitative and often quantitative agreement with the experimental data for NO, N_2O, and NO_2 emissions, and NH_3 slip in the whole equivalence ratio range, while allowing accelerated simulations compared to other leading mechanisms.

Received: 7th Jan 25; Accepted: 26th Mar 25; Published: 11th April 25

Keywords: Parameter optimisation, Laminar flame speed, Burner-stabilised stagnation flame, Jet-stirred reactor, Computational Fluid Dynamics

1. Introduction

The increasing concerns regarding oil resources and carbon dioxide (CO_2) emissions highlight the urgency to find alternatives to traditional liquid fossil fuels. Hydrogen (H_2) is seen as a promising alternative, however, its application raises safety concerns due to its volatility and low flash point [1]. In response to these challenges, using ammonia (NH_3) as a carbon-free fuel in combustion systems is gaining attention. It functions similarly to hydrogen in its role as a clean energy carrier and storage solution [1,2]. Additionally, storing and transporting NH_3 is relatively easier and safer than dealing with H_2 [2,3] due its extensive existing infrastructure, lower reactivity, and easier liquefaction, which also reduce overall costs compared to H_2 [4]. However, despite these advantages, the use of NH_3 in combustion presents notable challenges. Ideally, ammonia combustion should produce only nitrogen (N_2) and water (H_2O); however, in real-world applications, significant formation of nitrogen oxides (NO_x) is observed, especially under fuel-lean conditions [5]. NO_x refers to a group of compounds including nitrous oxide (N_2O), nitric oxide (NO), nitrogen dioxide (NO_2), dinitrogen trioxide (N_2O_3), and dinitrogen pentoxide (N_2O_5) [6]. Among these, N_2O, NO, and NO_2 have received considerable research attention due to their significant health and environmental impacts [6]. Other major drawbacks are its unfavourable combustion properties: low burning velocity and high ignition point. As a result, various techniques are employed to improve its combustion characteristics, one of which is blending with H_2 to enhance its overall combustion efficiency. Another important byproduct of concern is unburned NH_3,

* Corresponding author. Tel.: +44 2920 875948, +36 1 382 6507, E-mail address: ValeraMedinaA1@cardiff.ac.uk, nagy.tibor@ttk.hu
https://doi.org/10.18573/jae.46

particularly in fuel-rich mixtures of NH_3/H_2 blends. Similarly to NO_x species unburned NH_3 also has environmental and health challenges due to its toxicity and pollution potential [7].

To develop highly efficient and reliable combustion systems that produce minimal emissions, a full understanding of the chemical processes is needed, which can be achieved by developing kinetic reaction mechanisms. Numerous studies [8–28] have focused on developing kinetic models to accurately predict NH_3 combustion behaviour and emissions under a wide range of conditions. Many of these efforts utilise the mechanism of Miller and Bowman [29] as the core mechanism for improved kinetic models under specific conditions. Enhancing model accuracy involves either incorporating newly identified chemical reaction pathways [30], extending parameterization (e.g. with pressure dependence, enhanced third body efficiencies for additional species [31]), or tuning the rate parameters of specific key reactions based on improved theoretical calculations or experimental measurements [13,32,33]. Despite these efforts, discrepancies in the predictive performance of the improved kinetic models persist and require further investigation [34–36]. Chemical kinetic models are usually developed using quantum chemical method and statistical rate theory, with their kinetic parameters often manually tuned based on indirect experimental measurements of ignition delay times (IDT), laminar burning velocities (LBV), and concentrations in jet-stirred reactors (JSR), flow reactors (FR), and burner stabilised flames (BSF), whose simulation is relatively straightforward using either 0D or 1D reactor models. However, the development of modern combustion devices with intricate geometries and flow fields requires Computational Fluid Dynamics (CFD) simulations [37], which are computationally very demanding and thus can be run effectively only with small kinetic models. Consequently, the challenge in developing a reaction mechanism for CFD applications lies in achieving good predictive performance across various conditions and finding the balance between the complexity of the chemistry involved and its flexibility for CFD simulations with affordable computational costs. In detailed NH_3/H_2 mechanisms, the H/N/O kinetic system comprises over 30 species and around 200 reversible reactions, making CFD simulation computationally intensive. Simplifying the chemistry in kinetic models by including only the species and reactions relevant to specific conditions is a commonly used approach to reduce computational time [38–42].

Chemical Reactor Network (CRN) modelling allows approximate simulation of combustion systems with complex geometries by representing the flow field as a network of interconnected simple 0D reactors. CRN modelling allows a significant reduction in computational effort compared to CFD simulations, which enables the use of detailed kinetic models. Since the CRN is constructed based on CFD results and is usually tailored for specific results, it provides an efficient alternative for simulating NO_x chemistry in complex systems such as industrial gas turbine (GT) engines [43–48].

Early efforts to optimise kinetic parameters for combustion mechanisms were led by Frenklach et al. [49,50], followed by Sheen and Wang [51,52], Turányi et al. [53], and Pitsch and coworkers [54]. Building on the PrIMe data format of fundamental combustion experiments [55], Turányi and colleagues developed the ReSpecTh Kinetics Data (RKD) format [56], the ReSpecTh information system [57], and the Optima++ code [53,58,59], enabling the storage, simulation, and optimisation of combustion experiments across various fuel systems including hydrogen [60], H_2/NO_x [61] and ammonia [34,35].

The current work aims to develop a compact reaction mechanism for NH_3/H_2 blends with high predictive accuracy for laminar burning velocity and NO_x and NH_3 concentrations in CFD simulations by parameter optimization of the San Diego kinetic model [35]. The San Diego model was selected as a baseline for improvement due to its exceptionally small size (21 species and 64 reactions) and it showed good to satisfactory predictive performance over a wide range of conditions, based on the findings of Szanthoffer et al [35].

2. Methods

2.1 Kinetic model optimization

Accuracy of a combustion kinetic model can be characterised by an error function, which measures the deviation of the simulation results from the experimental data for a data collection. Turányi et al. proposed the following experimental uncertainty normalised mean square error function [53], and implemented into Optima++ for performance evaluation and parameter optimization of combustion kinetic models,

$$E(\boldsymbol{P}) = \frac{1}{N}\sum_{f=1}^{N_f}\sum_{s=1}^{N_{fs}}\frac{w_{fs}}{N_{fsd}}\sum_{d=1}^{N_{fsd}}\left(\frac{Y_{fsd}^{\mathrm{sim}}(\mathbf{P}) - Y_{fsd}^{\mathrm{exp}}}{\sigma(Y_{fsd}^{\mathrm{exp}})}\right)^2 . \quad (1)$$

N, N_f , N_{fs}, N_{fsd} are the number of data series in all RKD data files, the number of files, the number of data series in the f^{th} file, and the number of data in the s^{th} data series of the f^{th} file, respectively. Y_{fsd}^{exp} and $\sigma(Y_{fsd}^{\mathrm{exp}})$ are the d^{th} experimental data in the s^{th} data series of the f^{th} file and its one standard deviation

uncertainty, respectively. $Y_{fsd}^{\mathrm{sim}}(\mathbf{P})$ is the corresponding value simulated by the investigated kinetic model at vector of model parameter values **P**. If the experimental uncertainty of the measured data *y* can be characterised with relative error, e.g. in the case of IDTs, then logarithmic transformation $Y = \ln y$ is applied, as symmetric relative error spanning even orders of magnitude deviations can be represented as absolute error on natural logarithmic scale. The error function averages the squared normalised prediction errors of the mechanism within each data series, and in the case of $w_{fs} = 1$ (for all *f* and *s*), it weights each data series equally, so it is not biased by the different sizes of individual data series. In some cases, one might want to deviate from this approach, using non-unit w_{fs} weights either to emphasise more important data series or to correct biases arising from highly imbalanced data quantities or highly different magnitudes of errors for different types of experiments.

The predictive power of a combustion kinetic model can often be improved significantly by tuning their rate coefficients, or more specifically, the corresponding Arrhenius parameters. The current study utilises the highly efficient Optima++ code [53,58,59], which relies on the very robust FOCTOPUS optimization algorithm in tuning the Arrhenius parameters of rate constants within loose uncertainty limits [62,63] to fit the model predictions to experimental data collected from previous studies while considering the associated experimental uncertainties. The value of the error function has an absolute meaning, as $\sqrt{E}$ measures the uncertainty normalised root-mean-square deviation ("RMSD error") between the model and the experimental results, thus for the "perfect" model $\sqrt{E} \leq 1$, if $\sqrt{E} \approx 2$ the model is usually considered a great model, and a model is considered satisfactorily predictive if $\sqrt{E} < 3$. The error function can also be evaluated only for a part of the data collection, for example only for laminar burning velocities or concentrations of a given species, thus different aspects of the model performance can be assessed.

The influential reactions are usually identified by local sensitivity analysis of the simulation results with respect to the rate coefficients (e.g. A_j pre-exponential factors) [64], which ranks reactions based on their log-normalised local sensitivity coefficient,

$$S_{fsd,j} = \frac{\partial \ln Y_{fsd}^{\mathrm{sim}}}{\partial \ln P_j} \qquad (2)$$

The identified most important parameters are called the active parameters of the optimization, as their values are tuned to minimise the error function. There are more advanced methods, such as the PCALIN method [65] which was derived from the second-order Taylor expansion of the error function. As a results, it inherently accounts for the uncertainty of the rate coefficients and experimental data while also incorporating all normalization and weighting within the error function. This enables a more effective selection of parameters, leading to a more efficient improvement of the model.

Due to the small size of the San Diego 2018 mechanism compared to other detailed models that incorporate the latest theoretical findings (e.g. [24]), it inevitably misses important chemical species and pathways. Consequently, even if its rate coefficients had the physically exact temperature and pressure dependences, its performance would be suboptimal due to its mechanistic deficiencies. During the optimization of the reaction rate parameters, the uncertainty ranges of the rate coefficients of the individual elementary reactions determined by the present state of knowledge are disregarded. This approach allows us to expand the search range of the rate coefficient values to compensate for simulation errors caused by the incomplete chemical description. Therefore, a wide, ±1 order of magnitude uncertainty range was defined around the nominal rate coefficient curves in the temperature range of 500–2500 K. This assumed uncertainty corresponds to uncertainty parameter value $f = 1$, which was used in Optima++ for uniform sampling of ln*A*, *n* and *E*/*R* transformed Arrhenius parameters as proposed by Nagy et al. [63].

It is important to note that all the kinetic mechanisms for ammonia are still likely to be neither structurally nor parametrically complete. A key poorly described phenomenon is ammonia's role as a third body. In NH_3/H_2 combustion, NH_3 is a major component and a strong collider regarding energy transfer due to its multiple vibrational modes that effectively absorb and redistribute energy, as well as its strong intermolecular interactions, including dipole forces and hydrogen bonding, which enhance collisional deactivation and stabilization of reactive species. This leads to unusually large (e.g. 5–20 relative to N_2 or Ar) temperature-dependent third-body efficiencies, as supported by experimental and theoretical studies [66–68]. However, most mechanisms either neglect this or apply temperature-independent enhanced third-body efficiencies (e.g. Zhu 2024). Since no model fully captures NH_3 third-body effects yet, their accuracy is often achieved through off-tuned rate coefficients that compensate for these gaps.

Finally, the performance of the improved San Diego 2018 reaction mechanism developed in this study was evaluated by assessing its accuracy against 21

reaction mechanisms from the literature [8–28]. These mechanisms were selected based on their optimised performance, incorporating recent findings in kinetic modelling, such as corrections to the rate constants of key reactions in NH_3 kinetics and the inclusion of new NOx formation pathways. These advancements contribute to a more precise representation of ammonia combustion chemistry.

2.2 Experimental data and its uncertainty

To develop an improved model with robust performance for different burner designs, a large collection of NH_3/H_2 LBV, and concentration data measured in JSRs and burner-stabilised stagnation flames (BSSF) [69] were considered as optimisation targets. All JSR data and a large part of the LBV data have been collected and previously used for model performance evaluation by Szanthoffer et al. [35,70], encoded into RKD format data files [56], and stored in the ReSpecTh database [57]. The newly collected data (LBV and BSSF) has also been encoded into RKD files and are available in the ReSpecTh database with the publication. Each RKD file contains a single series of experiments, in which one or more properties are measured as a function of a systematically varied condition parameter, giving one or more data series, while other parameters are kept unchanged or varied only a little. In the case of LBV measurements, LBV is usually measured as a function of equivalence ratio (φ), in the case of JSR measurements, outlet concentrations of multiple species are measured as a function of temperature. In BSSF measurements, the outlet concentration is measured as a function of equivalence ratio. The total number of RKD files (N_{files}), experiments (N_{exp}), data series (N_{series}), and data points (N_{point}) and the covered ranges of conditions regarding hydrogen mole fraction in fuel blend (x_{H2}; same as volume fraction), equivalence ratio (φ), pressure (p), and unburnt gas temperature (T_u for LBV and BSSF) or temperature (T for JSR) are shown in Table 1. Our data collection is highly imbalanced as it contains 7 BSSF concentration, 47 JSR concentration, and 179 LBV data series.

Regarding BSSF measurements, only a single data series for 70 vol% ammonia and 30 vol% hydrogen mixtures was used, as measured by Hayakawa et al. [69]. The 70/30 vol% NH_3/H_2 mixture optimises combustion by combining ammonia's high energy density and carbon-free nature with hydrogen's fast flame speed and wide flammability range. This balance improves ignition, flame stability, and emissions performance, making it a promising clean fuel blend for engines and gas turbines [23]. There is significant disagreement in the experimentally measured concentration values obtained by different laboratories in JSR experiments with pure NH_3 fuel under the same experimental conditions. Therefore, such JSR experiments were ignored in this study, and only data for NH_3/H_2 mixtures, measured by Zhang et al. [23] and Osipova et al. [71], were considered. Nevertheless, the measurements of Zhang et al. [23] for NH_3/H_2 mixtures with 10-70 vol% H_2 content, spanning NH_3 concentrations from 90-30 vol%, encompass ammonia-dominant fuel blends, and thereby provide useful information on the chemical kinetics of ammonia blended turbulent flames. LBV measurements were available from 26 publications, listed in Table 2 which contains similar information as Table 1, and it also provides information on the applied experimental method used for determining LBV: OPF, HF, and FC stand for outwardly propagating spherical flame, heat flux and flame cone methods, respectively. Some experiments were discarded due to various reasons. From the JSR data series, three experiments were removed from both the Zhang et al. [23] and Osipova et al. [71] measurements, due to either enormous prediction errors across all mechanisms, or convergence issues during simulations. The 14 LBV measurements of Karan et al. [72] using OPF with the constant volume method provided 14 data series, each with a large number (from 37 to 291) of densely sampled LBV data points with unburnt gas pressure and temperature varying monotonically. These data series have significant redundancy; therefore, to avoid unnecessary simulations, each series was subsampled to have only 10 points (equidistantly by index), resulting in 140 points instead of 2102. LBV data which include measurements with helium bulk gas were not considered in this study, as it is not relevant for practical applications.

The present work focuses on model development for burners, where laminar and turbulent flame zones can be well approximated by 1D (freely propagating and/or burner-stabilised) laminar flame simulations and 0D jet-stirred reactor simulations, respectively.

Table 1. Optimisation targets from different reactor types used in the current study

Measurement	Publication	Ref.	N_{files}	N_{series}	N_{exp}	N_{point}	x_{H2}%	φ	p/atm	T or T_u/K
BSSF conc.	Hayakawa et al. 2022	[69]	1	7	17	119	30	0.57-1.40	1	298
JSR conc.	Zhang et al. 2021	[23]	8	14	71/74	284/296	10-70	0.15-0.79	1	800-1281
	Osipova et al. 2022	[71]	3	33	51/54	254/269	38-61	0.60-1.50	1	800-1300
LBV	See Table 2.	-	179	179	1283	1283	0-100	0.20-2.00	1.0-36.6	295-584
All	TOTAL	-	191	233	1416	1940	0-100	0.20-2.00	1.0-36.6	295-1281

Table 2. Laminar burning velocity measurement considered in the current study

#	Publication	Ref.	Method[a]	N_{XML}	N_{point}	x_{H2}%	φ	p/atm	T_u/K
1	Lee et al. 2009	[75]	OPF	5	10	10-50	0.6-1.67	1.0	298
2	Lee et al. 2010	[76]	OPF	3	15	69-100	0.6-1.67	1.0	298
3	Hayakawa et al. 2015	[77]	OPF	3	13	0	0.8-1.2	1.0-4.9	298
4	Ichikawa et al. 2015	[78]	OPF	3	22	0-100	1.0	1.0-4.9	298
5	Li et al. 2018	[79]	OPF	1	6	0	0.8-1.3	1.0	300
6	Han et al. 2019	[80]	HF	6	99	0-45	0.7-1.6	1.0	298
7	Liu et al. 2019	[81]	OPF	5	26	0	0.2-2.0	0.5-1.6	298
8	Mei et al. 2019	[82]	OPF	7	51	0	0.6-1.5	1.0-5.0	298
9	Han et al. 2020	[83]	HF	7	63	0	0.7-1.5	1.0	298-448
10	Lesmana et al. 2020	[84]	FC	3	21	0-8	0.9-1.2	1.0	295
11	Lhuillier et al. 2020	[85]	OPF	35	240	5-60	0.8-1.4	1.0	298-473
12	S. Wang et al. 2020	[86]	HF	5	67	40-60	0.6-1.6	1.0-4.9	298
13	D. Wang et al. 2020	[87]	OPF	9	51	0	0.6-1.4	1.0	303-393
14	Xia et al. 2020	[88]	OPF	2	15	0	0.6-1.6	1.0	298
15	Kim et al. 2021	[89]	OPF	3	12	0	0.9-1.2	1.0	298
16	Li et al. 2021	[90]	OPF	4	22	0	0.6-1.4	1.0	300
17	Mei et al. 2021	[24]	OPF	7	40	14-86	0.7-1.4	1.0-10.0	298
18	Osipova et al. 2021	[91]	FC	1	9	30	0.7-1.5	1.0	368
19	Shrestha et al. 2021	[92]	OPF	23	105	0-30	0.8-1.4	1.0-9.4	298-476
20	N. Wang et al. 2021	[93]	OPF	3	17	10-20	0.5-1.5	1.0-4.9	360
21	Gotama et al. 2022	[13]	OPF	2	14	40	0.8-1.8	1.0-4.9	298
22	Han et al. 2022	[94]	HF	4	49	4-60	0.6-1.6	1.0	298
23	Hou et al. 2022	[95]	OPF	6	32	0	0.7-1.3	1.0-14.8	298
24	Ji et al. 2022	[96]	OPF	10	92	0-87	0.6-2.0	1.0	303
25	Karan et al. 2022	[72]	OPF	14	140[b]	0	0.8-1.3	2.0-36.6	369-584
26	Zitouni et al. 2023	[97]	OPF	8	52	0-80	0.6-1.4	1.0	298

[a] OPF: Outwardly Propagating spherical Flame method, HF: Heat Flux method, FC: Flame Cone method.
[b] Originally published 2102 data points in 14 series were subsampled, resulting 10 points in each series.

However, to develop a more robust model for a wider range of applications, or to mimic the chemistry in certain smaller regions within the burner, concentration and ignition delay data from plug flow and micro flow reactors (e.g. Nakamura and co-workers [26]) could also be incorporated for parameter optimisation.

Experimental data uncertainty is an essential component of the error function (Eq. (1)); therefore, its estimation is a central issue in model evaluation and parameter optimization studies. Many authors often publish too optimistic uncertainty estimates, and the statistical noise of the data series is often larger than the published uncertainties. A method for the a posteriori assessment of statistical noise in a data series was developed and implemented into the Minimal Spline Fit code by Nagy and Turányi [73]. This code estimates the standard deviation of the statistical noise in an experimental data series ($\sigma_{fs,\mathrm{stat}}$ for the s^{th} data series in f^{th} RKD file) which was measured as a function of a single systematically varied condition parameter. The uncertainty published by the experimentalist ($\sigma_{fsd,\mathrm{exp}}$) and the statistical uncertainty ($\sigma_{fs,\mathrm{stat}}$) were assumed to be independent of each other and were combined using the following formula proposed by Olm et al. [74] to give a more conservative estimate for the uncertainty of the experimental data:

$$\sigma\left(Y_{fsd}^{\mathrm{exp}}\right) = \sqrt{\sigma_{fs,\mathrm{stat}}^2 + \sigma_{fsd,\mathrm{exp}}^2}\ . \qquad (3)$$

This procedure was followed by Szanthoffer et al. [35] and also in this work for the previously and newly collected experimental data.

2.3 Accelerated flame simulations

Sensitivity analysis, when dealing with many reactions in the model, and model optimization, when involving many active parameters, require numerous repeated simulations using the same mechanism with modified parameters. A comprehensive database of numerical simulation results is established in Optima++ to reduce the computational overhead of repeated simulations. In order to accurately account for the high relative diffusivity of hydrogen in NH_3/H_2 combustion, simulations were run considering multicomponent transport and thermal diffusion. Furthermore, to ensure the numerical accuracy, strict convergence

criteria with low gradient and curvature thresholds (0.02) were applied. It was recently shown by Nakamura et al. [27] and Stagni et al. [31] that the consideration of thermal radiation is also crucial for NH_3 flames [31]. Flame simulations of such quality could be done relatively quickly on a single core of a modern CPU (e.g. AMD Ryzen 9 7950X) for half of the laminar flame conditions with the San Diego mechanism using the Cantera 2.6 solver [98], which was employed in this study. However, a large part of the conditions required hundreds of seconds, and convergence issues were experienced (eight points did not converge even within ten minutes if thermal radiation was considered) even if the calculations were initialised using converged solutions under similar condition and fine sweeping was applied between their conditions. Given the large number of flame conditions (1283 experiments) and the extensive repeated simulations required for the optimization of several parameters, it was necessary to accelerate the simulations to ensure the optimization could be completed within a reasonable timeframe. Consequently, as a compromise between accuracy and fast simulations free from convergence issues, loose thresholds for gradient (0.06) and curvature (0.12) convergence criteria were employed and thermal radiation was neglected during optimization.

At these loose integrator thresholds, individual simulation results can sometimes exhibit significant variation (e.g., 20%). However, its effect is mainly stochastic and approximately symmetric, so when a large number of simulations are considered, the random deviations average out and cause little

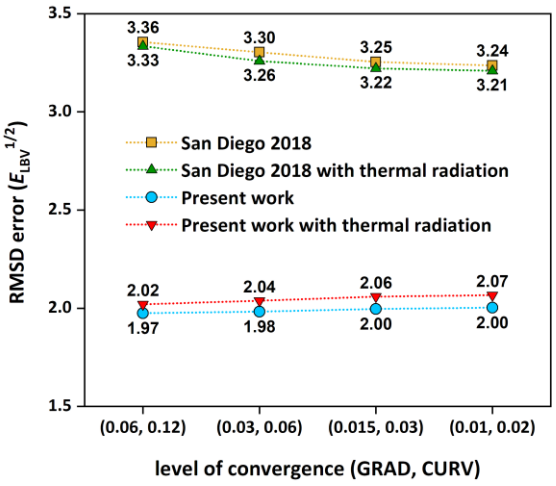

Fig. 1. Convergence of the error function for laminar burning velocities in the original and optimized San Diego 2018 models, with and without thermal radiation. Level of convergence is increased by tightening the relative gradient (GRAD) and curvature (CURV) thresholds in flame simulations.

change in the overall error. To validate the applicability of this approximation for model optimization, a convergence analysis was performed on the error function value of freely propagating laminar flame simulations using both the original San Diego 2018 mechanism and the optimised model (present work), with and without thermal radiation. As shown in Figure 1, tightening the relative thresholds for gradient and curvature led to high-accuracy convergence of the overall RMSD error function for laminar burning velocities from 1283 simulations. The plot indicates a maximum deviation of 0.12 in the overall LBV RMSD error value (e.g. 3.36-3.24) due to the high applied thresholds and up to 0.7 due to the neglect of thermal radiation (e.g. 2.07-2.00). These inaccuracies are very small compared to the decrease in the error function at the tightest thresholds with thermal radiation considered (3.21→2.07). Similarly small variations are expected for other literature mechanisms, which would have only a minor impact on their predictivity ranking (see later in Table 4.). Thus, it is an acceptable trade-off, as significantly larger improvements are realised following parameter optimization. The time required to evaluate the performance of the San Diego mechanism with a modified parameter set reduced to 110 s on the whole data collection (32 threads of an AMD Ryzen9 7950X CPU with 64GB of DDR5 RAM, and a fast NVME M.2 SSD drive), which enabled fast optimization.

When sensitivity analysis is conducted with loose convergence thresholds, the added noise in the solution can result in significant sensitivity coefficients even for non-influential reactions. This noise is partially cancelled if the solution for the perturbed model is initialised from the solution of the unperturbed model (i.e., the noise is partially inherited) and can be further dampened by applying large perturbations (e.g., factors of 2 or 5). However, in the present study, due to the limited number of rate coefficients (a total of 69 low- and high-pressure limits across 64 reactions), brute-force sensitivity analysis of LBV calculations could be performed at tight convergence thresholds (GRAD = 0.01, CURV = 0.02) within a reasonable timeframe, without incorporating thermal radiation.

2.4 CFD simulations

This section describes the numerical setup for the computational fluid dynamics (CFD) simulation of a turbulent swirl flame, with a constant burning power of 10 kW and selected equivalence ratios of 0.6, 0.8, 1.0, and 1.2. The novel burner geometry and experimental setup were presented in detail by Mashruk et al. [99]. The raw experimental data from [99] were standardised using the averaged oxygen

and water content and presented as 15 vol% O_2 on a dry gas basis. The simulations were conducted using Ansys Fluent 2024r1 [100] with the Reynolds-averaged Navier-Stokes (RANS) approach and the Reynolds Stress Model (RSM) for turbulence. The Stress-Menters Baseline (Stress-BSL) model was selected to represent the pressure-strain term in the transport equation for stresses. It improves standard omega closure by removing the sensitivity to free-stream sensitivity conditions, enabling more accurate modelling of complex swirling flows. Although it offers potential improvements, it is important to note that the model may inherit certain limitations of omega-based models. The reacting flow calculations used the Eddy Dissipation Concept (EDC) combustion model. Calculations were performed using the default turbulent Schmidt number value (0.7) and including thermal diffusion.

The calculations included the determination of heat transfer rates for the burner and quartz glass at a temperature of 288 K, with and a heat transfer coefficient of 20 W/m²K. The radiative heat flux was modelled using the Discrete Ordinates (DO) model.

In consideration of the heat and flow models applied, the coupled pressure-velocity solver was employed with the Procedure for Efficient Solution of Transient and Steady-State Operations (PRESTO!) scheme for pressure discretization, and a second-order scheme was used for the remaining equations.

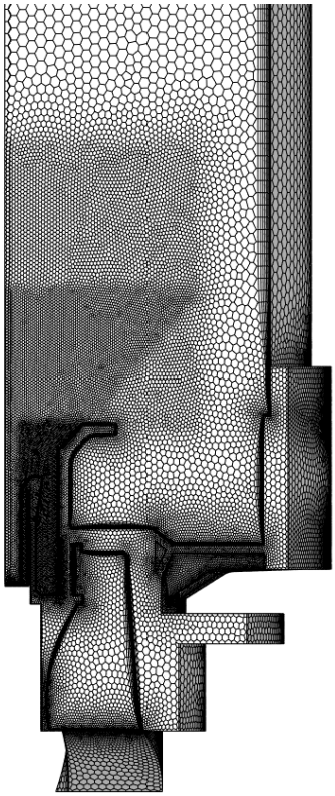

Fig. 2. Radial cross-section of a 40-degree periodic burner section showing the computational grid structure and domain configuration.

The improved mechanism presented in this work was compared to the Stagni et al. 2020 [28] and Nakamura et al. 2019 [27] mechanisms, which were selected for their relatively small size, overall good performance, and very good predictive capability for emissions in rich ammonia-hydrogen flames [101,102]. In view of the relatively high projected heat loss to the ambient through the quartz wall, the available data on non-adiabatic stagnation flames were analysed and selected, with a primary focus on NO emissions, followed by N_2O. Valuable insights into NO emissions predictions for BSSF modelling were presented in [103]. In rich conditions, the Stagni 2020 mechanism [28] demonstrated one of the best agreements for the BSSF model, while underestimating NO emissions in lean conditions. The Nakamura 2019 mechanism [27] demonstrated superiority in lean to stoichiometric conditions, exhibiting greater divergence in rich mixtures. Nevertheless, none of the mechanisms investigated in reference [103] were capable of reproducing the NO emission across the entire equivalence ratio range. Consequently, two mechanisms were selected for comparison with PW mechanism results. It is noteworthy that similar trends were observed in the CFD emission results, although the absolute differences were considerably smaller for the modelled turbulent flame than the 1D laminar flame.

A 40-degree rotationally periodic section of the combustor above was represented with a three-dimensional mesh of 1.6 million polyhedral elements for a radial cross-section (see Fig. 2). Simulations were carried out for a fully premixed mode of the burner operation, which allowed the mesh size to be reduced but neglected possible inhomogeneities in the H_2 distribution, which in the experimental setup is supplied near the tangential swirler for safety reasons. A significant densification of the grid was performed for the region surrounding the projected flame position, the tangential swirler and the boundary layer near possible separation points.

2.5 Chemical Reactor Network

Chaturvedi and coauthors have recently developed a Chemical Reactor Network (CRN) model [44] to investigate the NO_x chemistry in experimental swirling NH_3/H_2 flames. This development is based on using CFD simulations to model the reacting flow field of a 70/30 vol% NH_3/H_2 blend in a generic swirl burner geometry developed at the Thermofluids Lab at Cardiff University [104].

Table 3. Kinetic mechanisms used for comparison in CRN modelling

#	Mechanism	Ref.	N_{spec}	N_{reac}
1	Lamoureux 2010	[105]	119	883
2	Nakamura 2017	[33]	33	232
3	Glarborg 2018	[21]	39	231
4	Klippenstein 2018	[20]	33	211
5	Stagni 2020	[28]	31	203
6	Han 2021	[106]	36	298
7	Zhang 2021	[23]	38	263
8	Glarborg 2022	[15]	41	270
9	Present work (PW)	-	21	64

The computational domain was divided into zones based on the velocity field and the uniformity of temperature and species. The flame region was divided into seven main zones, each corresponding to a specific temperature range and individually modelled using Perfectly Stirred Reactors (PSRs) to capture their unique characteristics. The velocity field was defined by two recirculation zones, the Central Toroidal Recirculation Zone (CTRZ) and the Edge Recirculation Zone (ERZ), which are distinctive features of swirl flows in swirl-stabilised combustors and were modelled using PSRs. Finally, a Plug Flow Reactor (PFR) represented the burner exit zone. For further details, please refer to [44].

The developed CRN model will be used to evaluate the performance of the improved kinetic reaction mechanism and compare its predictive performance against the performance of eight kinetic models as detailed in Table 3. These models have been recognised in recent studies [102,103,107,108] for their accuracy in predicting the chemistry of NO [103], N_2O [102], NO_2 [107], and unburned NH_3 [108] across various equivalence ratios for a 70/30 vol% NH_3/H_2 flames. Furthermore, the model's predictions will be validated against experimental measurements conducted using the same swirl burner employed for CRN model development, under similar fuel blend and atmospheric conditions [104].

3. Results

3.1 Kinetic model optimization

In addition to the San Diego 2018 mechanism, 20 NH_3/H_2 mechanisms published since 2018 were collected from the literature to evaluate the performance of the optimised model in comparison with the most accurate models currently available. As the simulated experiments contained no carbon atom containing species, all such species and their reactions were removed from all mechanisms to make a fair comparison of their size and accelerate simulations. The list of the considered 21 literature ("decarbonised") mechanisms, together with the number of species (N_{spec}) and reactions (N_{reac}), are shown in Table 4. The table shows that most mechanisms have 31–35 species and 160–240 reactions. The most detailed mechanisms were published by Meng et al. [19] and Zhu et al. [8] which have 269 and 312 reactions, respectively. The

Table 4. Size and prediction errors of the investigated NH_3/H_2 kinetic models in various combustion systems

#	Mechanism[a]	Ref.	N_{spec}[b]	N_{reac}[b]	$\sqrt{E_{LBV}}$[c]	$\sqrt{E_{JSR}}$[c]	$\sqrt{E_{BSSF}}$[c]	$\sqrt{E_{Overall}}$[c, d]
1	**Zhu 2024**	[8]	39	312	2.97	1.11	2.27	2.25
2	**Han 2023**	[9]	32	171	2.24	1.63	3.70	2.67
3	**Present work**	-	21	64	1.97	2.72	3.24	2.70
4	**Jian 2024**	[10]	32	233	3.23	1.80	3.79	3.06
5	**Otomo 2018**	[11]	32	213	3.67	2.03	3.65	3.21
6	**X. Zhang 2021**	[23]	34	224	2.45	2.78	4.59	3.41
7	**Stagni 2023**	[12]	31	203	3.46	1.75	4.69	3.51
8	**Gotama 2022**	[13]	32	165	3.28	2.91	4.59	3.67
9	**Nakamura 2019**	[27]	34	229	3.75	2.87	4.71	3.85
10	**Stagni 2020**	[28]	31	203	3.32	3.31	4.90	3.91
11	**Liu 2024**	[14]	35	238	3.96	2.39	5.19	4.01
12	**Glarborg 2022**	[15]	34	227	6.42	2.55	4.45	4.74
13	**Glarborg 2023**	[25]	34	228	6.52	2.54	4.45	4.79
14	**He 2023**	[16]	34	221	7.37	2.46	4.45	5.17
15	**Z. Zhang 2024**	[17]	34	224	8.46	1.14	4.50	5.57
16	**Mei 2021**	[24]	35	239	4.02	1.65	9.84	6.21
17	**Wang 2022**	[18]	32	140	2.53	2.64	10.13	6.22
18	**Tamaoki 2024**	[26]	33	228	3.29	2.14	10.17	6.29
19	**Meng 2023**	[19]	39	269	10.14	3.11	4.62	6.68
20	**Klippenstein 2018**	[20]	33	108	10.28	3.03	4.73	6.76
21	**Glarborg 2018**	[21]	33	211	10.29	3.03	4.73	6.77
22	**San Diego 2018**	[22]	21	64	3.36	2.43	13.94	8.40

[a] Mechanism denoted by first author and the year of publication, except for San Diego 2018 [22] and the Present work mechanisms.
[b] Green-yellow-red highlighting of cells corresponds to the minimum, the median and the maximum values, respectively.
[c] Green-yellow-red highlighting of cells corresponds to $\sqrt{E}$ = 2, 3, and 4 error values, respectively.
[d] Root mean square of the $\sqrt{E}$ errors for the three experiment types.

San Diego 2018 mechanism is the smallest in size, and even the next smallest mechanisms (e.g. Stagni 2023, Klippenstein 2018) contains at least ten more species and forty more reactions, which made their flame simulations even more challenging. Nevertheless, it was possible to carry out all flame simulations with them using the approximate description. However, for most of them, accurate calculations had convergence issues for a large fraction of the collection experiments.

To identify influential reactions whose rate coefficients should be optimised, sensitivity analysis was carried out on the whole data collection using +5% perturbation on the pre-exponential factor of all rate coefficients (64, and an additional 5 for low-pressure limit rate coefficients). Sensitivity analysis showed that each of the 69 rate coefficients had a significant influence on the simulation results. The more sophisticated PCALIN method which directly assesses the variation of the error function upon variation of the parameters within their uncertainty ranges, also confirmed that all reactions can have significant influence if ±1 order of magnitude variation was allowed for their pre-exponential factor. Consequently, all rate coefficients were considered in the optimization, and all three Arrhenius parameters of them were tuned to exploit maximum flexibility of the model to compensate for the mechanistic deficiencies. During optimization, the error function weights in Eq. (1) were set to 1/179, 1/47 and 1/7 for the 179 LBV, 47 JSR and 7 BSSF data series, respectively, to compensate for the imbalance in the data collection. The optimised mechanism is included as supplementary material.

To characterise the model performance, the error function in equation (1) was evaluated separately for the three experimental data types using unit weights. Table 4 presents the performance of the 21 literature mechanisms and the optimised San Diego 2018 mechanism (Present work, PW mechanism) in terms of the square root error function values (i.e. $\sqrt{E}$, see Eq. (1) for *E*). $\sqrt{E}$ was evaluated for LBV, BSSF concentration and JSR concentration measurements separately, and the overall error function value ($\sqrt{E_{\text{Overall}}}$) was calculated as the root mean square average of the three errors. This way, each type of experiment has equal weight in the $\sqrt{E_{\text{Overall}}}$ values. The mechanisms are ranked according to the overall error.

The accuracy of the PW mechanism was greatly improved compared to the San Diego 2018 mechanism in predicting LBVs of NH_3/H_2 mixtures (including pure NH_3 and H_2). Surprisingly, it has become the most accurate mechanism for LBV calculation despite its smallest size. The mechanism predicts 85% of the available LBV data within 3σ experimental uncertainty. Very good performance is

Table 5. Prediction errors of the investigated kinetic models for BSSF and JSR concentration measurements

#	Mechanism[a]	Ref.	$\sqrt{E_{\text{JSR}}}$ [b]								$\sqrt{E_{\text{BSSF}}}$ [b]							
			NH_3	H_2	O_2	H_2O	N_2	NO	N_2O	RMS[c]	NH_3	H_2	O_2	H_2O	NO	NO_2	N_2O	RMS[d]
1	Zhu 2024	[8]	2.1	0.8	0.8	1.4	0.6	0.4	0.5	1.1	0.9	0.9	1.3	1.9	0.7	1.5	5.2	2.3
2	Han 2023	[9]	2.5	0.8	0.6	1.3	0.9	0.7	2.8	1.6	1.1	5.4	0.7	3.9	6.3	3.0	1.0	3.7
3	Present work	-	4.0	2.3	2.9	3.3	2.7	1.3	1.5	2.7	0.7	5.6	0.8	3.9	1.5	3.6	3.2	3.2
4	Jian 2024	[10]	2.2	2.6	1.0	1.3	2.8	0.5	0.5	1.8	1.8	5.1	0.7	4.0	2.8	2.2	6.5	3.8
5	Otomo 2018	[11]	2.9	1.4	2.5	2.3	2.4	0.5	1.0	2.0	0.8	5.3	0.8	3.8	5.4	1.9	4.1	3.7
6	X. Zhang 2021	[23]	3.5	2.8	1.3	3.1	3.5	1.1	3.0	2.8	1.3	5.6	0.7	3.8	3.9	2.8	8.7	4.6
7	Stagni 2023	[12]	2.0	1.3	0.8	1.8	2.1	0.6	2.7	1.8	1.5	5.4	0.7	4.0	3.3	2.7	9.4	4.7
8	Gotama 2022	[13]	2.9	3.7	2.1	2.4	1.2	1.2	5.0	2.9	1.0	5.6	0.7	3.8	5.1	3.1	8.1	4.6
9	Nakamura 2019	[27]	3.9	3.6	0.9	4.2	3.0	0.6	1.4	2.9	2.7	5.3	0.7	4.0	2.7	2.7	9.4	4.7
10	Stagni 2020	[28]	2.0	1.3	0.5	1.6	1.5	0.7	8.1	3.3	1.1	5.7	0.7	3.8	7.2	2.8	7.6	4.9
11	Liu 2024	[14]	2.7	1.4	1.4	2.7	1.1	1.2	4.3	2.4	1.5	5.5	0.7	3.9	6.2	3.2	9.6	5.2
12	Glarborg 2022	[15]	3.1	2.4	1.2	2.8	3.2	1.4	2.9	2.5	2.1	5.3	0.8	4.1	1.8	2.2	9.0	4.4
13	Glarborg 2023	[25]	3.1	2.4	1.2	2.8	3.2	1.4	2.9	2.5	2.2	5.3	0.8	4.0	1.8	2.2	9.0	4.4
14	He 2023	[16]	3.2	2.7	1.1	2.7	3.1	1.0	2.4	2.5	2.9	4.1	0.8	3.9	2.5	2.3	9.3	4.4
15	Z. Zhang 2024	[17]	2.1	0.6	1.1	1.5	0.6	0.5	0.4	1.1	3.1	4.1	0.7	4.0	2.9	2.4	9.2	4.5
16	Mei 2021	[24]	2.3	1.7	2.0	1.6	1.8	0.6	0.8	1.6	17.1	6.1	9.4	10.4	1.8	3.6	11.6	9.8
17	Wang 2022	[18]	3.6	3.5	2.7	3.0	2.0	1.5	0.9	2.6	17.2	8.2	9.3	10.9	5.1	3.8	10.5	10.1
18	Tamaoki 2024	[26]	2.9	1.2	2.3	1.8	2.3	1.8	2.3	2.1	17.2	8.2	9.3	10.8	5.7	3.8	10.5	10.2
19	Meng 2023	[19]	4.1	2.4	1.6	4.1	3.6	1.3	3.4	3.1	2.9	5.1	0.8	4.1	2.5	2.4	9.3	4.6
20	Klippenstein 2018	[20]	4.1	2.4	1.6	4.1	3.6	1.3	2.8	3.0	2.9	5.1	0.8	4.2	2.9	2.2	9.6	4.7
21	Glarborg 2018	[21]	4.1	2.4	1.6	4.1	3.6	1.3	2.8	3.0	2.9	5.1	0.8	4.1	2.9	2.2	9.6	4.7
22	San Diego 2018	[22]	2.8	3.1	1.1	3.1	1.0	0.7	3.4	2.4	24.9	10.1	12.3	15.8	9.7	5.5	10.7	13.9

[a] Mechanism denoted by first author and the year of publication, except for San Diego 2018 [22] and the Present work mechanisms.
[b] Green-yellow-red highlighting of cells corresponds to $\sqrt{E}$=2, 3, 4 error values, respectively.
[c] Root mean square of the data series $\sqrt{E}$ errors. The number of data series for the different species is not the same.
[d] Root mean square of the species $\sqrt{E}$ errors - there is only one data series for each species.

shown also by Han 2023 and the Z. Wang 2022 mechanisms, but the simulations using these mechanisms take at least five times longer than those using the PW mechanism.

The average performance in predicting JSR concentrations for NH_3/H_2 mixtures with at least 10 vol% H_2 content is acceptable for all models. Notably, the Zhu 2024 and Z. Zhang 2024 mechanisms provided especially accurate descriptions ($\sqrt{E} \sim 1$). Additionally, the Han 2023, Mei 2021, Stagni 2023, Jian 2018, Otomo 2018, and Tamaoki 2024 mechanisms performed well ($\sqrt{E} \sim 1.5$–2.1). The San Diego 2018 mechanism shows fair performance with $\sqrt{E} = 2.43$, with slight deterioration upon optimization ($\sqrt{E} = 2.72$), yet its error remains below 3.

In predicting BSSF concentration data, except for the most detailed Zhu 2024 mechanism ($\sqrt{E} = 2.27$), all mechanisms had unsatisfactory performance ($\sqrt{E} \geq 3.65$). While the San Diego 2018 mechanism had the highest error value of $\sqrt{E} = 13.9$, the PW mechanism emerged as the second-best one among the 22 mechanisms with $\sqrt{E} = 3.24$ for BSSF. Table 5 shows the prediction errors of the mechanisms for the concentrations of different species measured in JSR and BSSF experiments. Regarding JSR experiments, the PW mechanism has very accurate predictions for NO and N_2O ($\sqrt{E} \leq 1.5$), and acceptable predictions for H_2, O_2, H_2O and N_2. Its accuracy for NH_3 deteriorated significantly compared to the San Diego 2018 model ($\sqrt{E} = 2.8 \rightarrow 4.0$), however, surprisingly, none of the mechanisms can perform excellently in this regard (all $\sqrt{E} \geq 2$). Good descriptions are given only by the Stagni 2020, Stagni 2023, Zhu 2024, Z. Zhang 2024 and Jian 2024 mechanisms. Regarding NO emissions, all mechanisms perform well or excellently. For N_2O, only eight mechanisms, including the PW mechanism, can give accurate estimates ($\sqrt{E} < 2$), and five models, including the San Diego 2018 mechanism were unreliable ($\sqrt{E} \geq 3.4$. For O_2 concentrations, almost all mechanisms perform accurately, and four mechanisms, including the PW model, have acceptable performance. For H_2 concentrations, the predictions are also generally good or at least acceptable, and only the Gotama 2022, Nakamura 2019, Wang 2022, and San Diego 2018 mechanisms have unacceptably large errors ($\sqrt{E} > 3$). In summary, three mechanisms: the Zhu 2024, the Z. Zhang 2024, and the Mei 2021 mechanisms showed reliable performance for all seven species.

Regarding BSSF concentration measurements, the Zhu 2024 mechanism clearly stands out with its universal high accuracy for all species apart from N_2O. For H_2 and H_2O, all other mechanisms give bad predictions ($\sqrt{E} \geq 4.1$ and 3.8). For N_2O, only the Han 2023 ($\sqrt{E} = 1$) and PW ($\sqrt{E} = 3.2$) mechanisms show good and acceptable performances, respectively, whereas all other mechanisms perform poorly ($\sqrt{E} \geq 4.1$). Except for four mechanisms (Mei 2021, Wang 2022, Tamaoki 2024, San Diego 2018), all models give good or acceptable predictions for NH_3, with the PW emerging as the best. The trend is similar for O_2: all mechanisms, except for the same four models, give excellent predictions. These four bad performing mechanisms and the PW model are also inaccurate ($\sqrt{E} \geq 3.6$) for NO_2, whereas most models predict it relatively accurately or at least acceptably with an error of $\sqrt{E} = 1.9$–3.2. After Zhu 2024, the PW model has the best performance for NO ($\sqrt{E} = 1.5$), whereas half of the mechanisms perform badly ($\sqrt{E} \geq 3.0$).

3.2 CFD simulations

The CFD simulations of 70/30 vol% NH_3/H_2 mixture were carried out for a swirl burner at 0.6, 0.8, 1.0. and 1.2 equivalence ratios. In the simulations, the tested mechanisms provided similar flow fields and temperature distributions across all the tested equivalence ratios. Figure 3 summarises the simulation result for outlet concentrations of NH_3 and the three main NO_x species obtained by the three mechanisms in comparison with the experimentally measured values. Emissions are normalised to a reference oxygen concentration of 15 vol% in the dry exhaust, which excludes water vapor.

Regarding NO emissions in the $\phi = 0.8$–1.2 range, all mechanisms perform qualitatively well, with the Stagni 2020 mechanism demonstrating the best accuracy, whereas the other two significantly overpredict peak NO emissions in almost perfect agreement with each other. While all mechanisms demonstrated the highest NO emission at 0.8, the NO emission drop observed at very lean conditions was only captured by the improved mechanism. At very lean conditions, the PW mechanism predicts NH_3 slip accurately, whereas the other two mechanisms predict no slip at all. All mechanisms accurately describe the complete consumption of NH_3 under stoichiometric and slightly lean conditions, and they give a good qualitative description for the unburnt ammonia in rich flames.

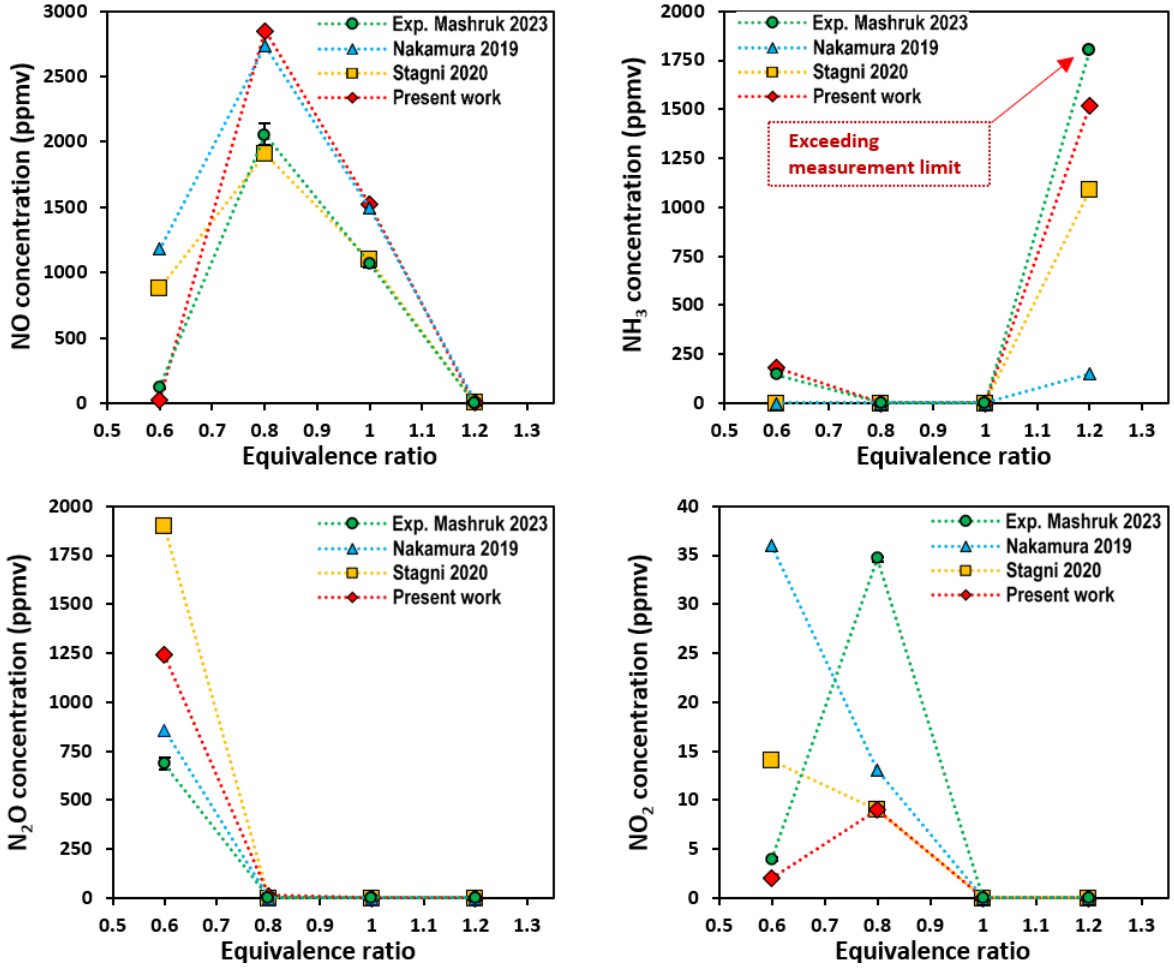

Fig. 3. Outlet concentration of NH_3, NO, N_2O, and NO_2 species measured experimentally by Mashruk et al. [99] and calculated using CFD simulations with three mechanisms (PW: present work) for 70/30 vol% NH_3/H_2 blends in a swirl burner design. Emissions are normalised to 15 vol% O_2 concentration in the dry exhaust (i.e. excluding water vapor). The results are connected by dotted lines only to make them easier to find and compare.

In the latter case, considering that experimental NH_3 emissions exceed the measurement limits, the present mechanism and the Stagni 2020 mechanism provide the best and second-best predictions, while the Nakamura 2019 model underpredicts the result by at least one order of magnitude. Regarding N_2O concentration predictions, all mechanisms are qualitatively correct as they give zero emissions only in the ϕ = 0.8–1.2 range. The Nakamura 2019 mechanism is the most accurate, with 20% overprediction, whereas the PW mechanism and the Stagni 2020 mechanism overpredict by 80% and 170%, respectively, compared to the experiment. Regarding NO_2 concentration all models reproduce zero emissions at stoichiometric and rich conditions. All mechanisms predict the emergence of emission at ϕ=0.8, however, they yield 3-4 times lower values than the experimental data. The Nakamura 2019 and the Stagni 2020 mechanisms give monotonically increasing emission with decreasing equivalence ratio, while the PW mechanism accurately captures the decreasing trend under very lean conditions.

In summary, the PW model captures the NH_3 slip and the rapid NO decrease at an equivalence ratio of 0.6, and it also shows good qualitative agreement with the N_2O and NO_2 concentrations. It should be noted that the resulting NO_2 emissions were under-predicted, falling within the range of a few ppm, so this trend requires further investigation for confirmation. However, given the limited number of data points, especially in regions with large gradients, such as very lean and near stoichiometric conditions, these predictions should be viewed as an indication of the mechanism's capabilities rather than a direct fit.

Figure 4 presents contour plots of the temperature and the NO concentration field, calculated with the Nakamura 2019 and present work mechanisms for φ = 0.8 lean conditions in a radial cross section of the burner. The most intense NO formation was observed on the inner side of the central recirculation zone and the flame tip.

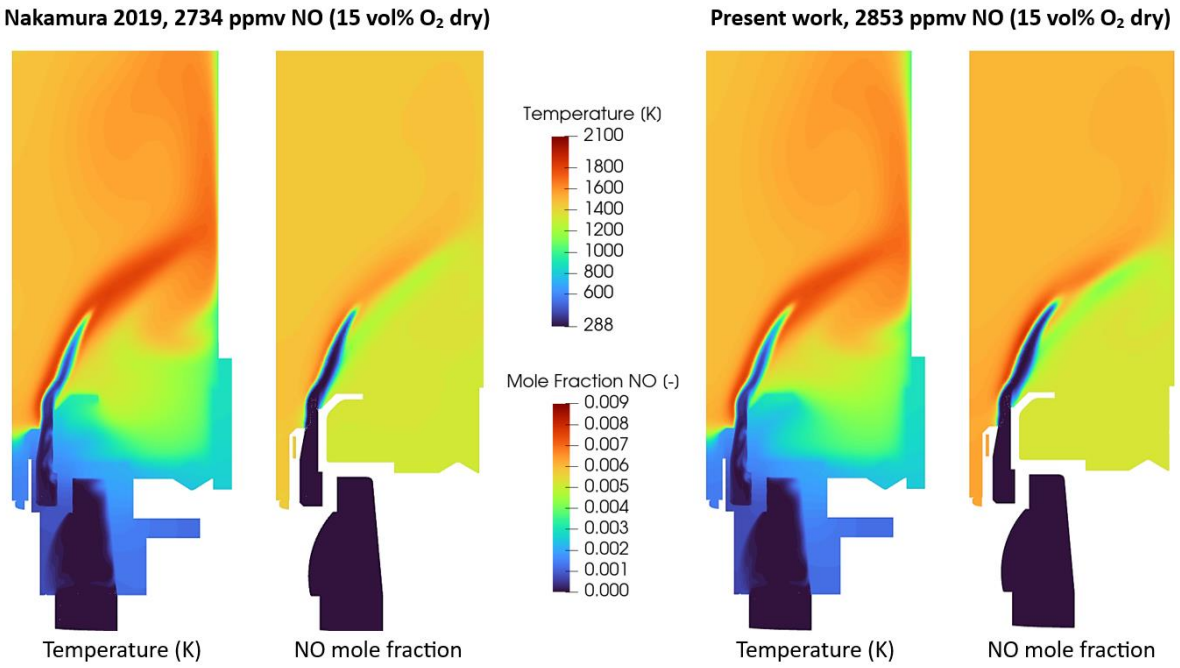

Fig 4. Contour plots of temperature and NO mole fraction φ=0.8 for 70/30 vol% NH_3/H_2 blend in a radial cross-section of a swirl burner obtained using CFD simulation with the Nakamura 2019 and present work mechanisms.

In contrast, a reduction was observed in the external recirculation zone, strongly correlated with the lower temperature region adjacent to the burner wall.

The NO and temperature contours for both mechanisms are largely similar, suggesting comparable performance in predicting the temperature profile and NO formation rates. This indicates that the PW mechanism effectively captures key NO formation characteristics despite employing less detailed chemical pathways compared to the Nakamura 2019 mechanism.

Additionally, it was found that all models were sensitive to changes in heat flux. A precise definition of the total heat transfer rates is essential, and while these rates are generally satisfactory, they may be underestimated for quartz walls due to the opacity of the walls. The results for the bottom of the burner were slightly overestimated, resulting in quenching and subsequent ammonia slip.

The key advantage of the PW mechanism is its computational efficiency, as it could be simulated 1.78 and 2.14 times faster than the Nakamura 2019 and Stagni 2020 mechanisms, respectively. The total simulation time for one case using 96 CPU cores was 7.5 hours with the PW mechanism and 16 hours for the Stagni mechanism. This improved efficiency is particularly notable, considering the good qualitative prediction of pollutant emissions achieved by the PW mechanism.

3.3 CRN simulations

A Chemical Reactor Network model, developed for another swirl burner based on CFD simulations of 70/30 vol% NH_3/H_2 mixtures to predict NO emissions, was employed to assess the accuracy of various kinetic models (see Table 3). The simulated NO concentrations and those of other major pollutants (NH_3, N_2O, NO_2) in comparison with experimental results over a wide range of equivalence ratios are shown in Figure 5.

The CRN design can describe NO concentrations qualitatively well with all mechanisms, with the Stagni 2020 and the Nakamura 2017 models being the most accurate regarding the maximum and the position of the NO peak. The PW model together with Glarborg 2022 and X. Zhang 2021 models predict higher peak NO emissions and at lower equivalence ratios. The Nakamura 2017 model at rich conditions shows an artifact of sudden steep rise of NO emissions, whereas the other models capture the decreasing trend of NO correctly.

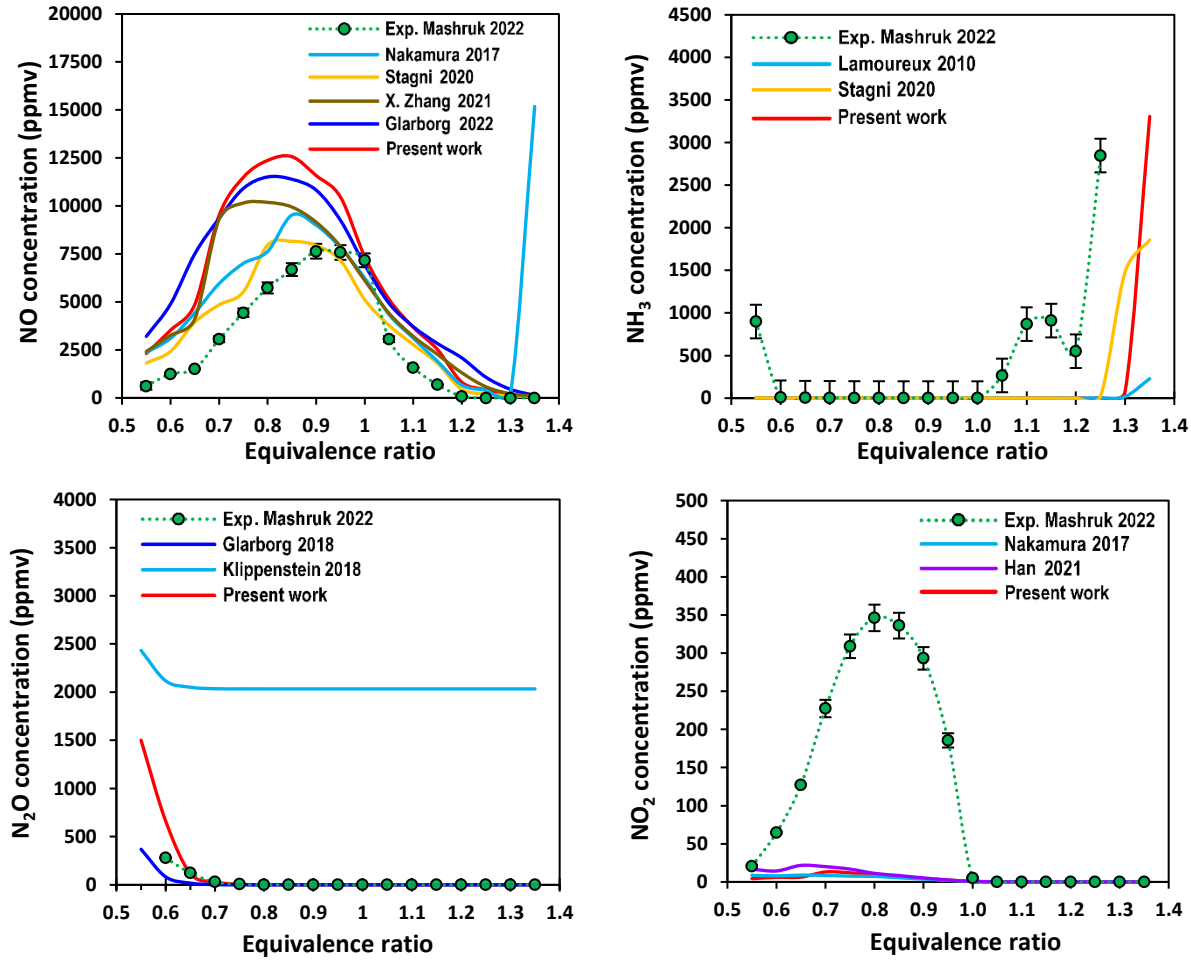

Fig. 5. Outlet concentration of NH_3, NO, N_2O, and NO_2 species measured experimentally by Mashruk et al. [104] and calculated using CRN with various mechanisms (P.W. Mech: present work) for 70/30 vol% NH_3/H_2 blends in a swirl burner design. Emissions are normalised to 15 vol% O_2 concentration in the dry exhaust. Simulation results were calculated at dense equivalence ratio values and therefore are represented with lines. The experimental results are connected by dotted lines only to make them easier to find and compare.

Regarding off-design species, the CRN design cannot capture NH_3 slip at lean conditions with any of the tested models, while at rich conditions the present optimised model can qualitatively reproduced the steeply increasing concentration trend. N_2O concentrations are captured qualitatively well with the Glarborg and the PW models, while the Klippenstein model predicts large emissions at all concentrations. NO_2 emission are badly underpredicted by the tested models, nevertheless the PW model predicts its peak at similar equivalence ratios.

In summary, this study also highlights the limitations of the CRN framework in predicting off-design species concentration due to its simplified methodology. Key factors such as residence time [109] and the local fuel-air equivalence ratio [110] must be incorporated, as relying solely on temperature profiles proves inadequate. Addressing these gaps offers a pathway for advancing CRN-based modelling approaches.

4. Conclusions

The optimised San Diego 2018 mechanism is the smallest NH_3 mechanism available and has the shortest computation time for flame simulations. However, due to its small size it inevitably misses important chemical pathways, and its performance in predicting laminar burning velocities (LBV) and concentrations in jet-stirred reactors (JSR) and burner-stabilised stagnation flames (BSSF) is only fair. In this study, it was found that the accuracy of the San Diego 2018 mechanism could be greatly improved by rate parameter optimization if unphysically wide tuning ranges are allowed for its rate coefficients. The optimised model showed the best performance for LBV and gave reliable predictions for NH_3, NO and N_2O in BSSF and for

NO and N_2O in JSR, but its performance for NO_2 in BSSF and for NH_3 in JSR still needs to be improved. The model has also been tested in computational fluid dynamics simulations of a swirl burner, and it allowed rapid simulations there as well. Its predictions showed excellent qualitative and often good quantitative agreement with the experimentally measured emissions, which could not be provided by other widely used mechanisms.

Despite the greatly improved performance of the optimised San Diego 2018 model, it is clear that the lack of potentially important reaction pathways can only be partially compensated for by tuning the rates of other reaction pathways. Possible development directions can be the extension of its chemistry with a few species and a few dozen reactions and the extension of its parameterization, as the pressure-dependent description and relevant third body efficiencies, especially for NH_3, are missing for some important reactions.

Owing to the significant structural deficiencies of the San Diego 2018 model, the optimised rate parameters should by no means be considered as recommended physical values. Nevertheless, the optimised kinetic mechanism offers a good compromise between predictivity and computability and can thus serve as a useful model for developing practical applications using CFD simulations.

Acknowledgments

The authors express their gratitude for the support received from EPSRC through the SAFE-AGT Pilot project (No. EP/T009314/1) and the Green Ammonia Thermal Propulsion MariNH3 project (No. EP/W016656/1). Ali Alnasif also extends his thanks to Al-Furat Al-Awsat Technical University (ATU) for financially supporting his PhD studies in the U.K. T. Nagy and T. Turányi thank the support of the National Research, Development, and Innovation Fund (NKFIH) FK134332 and K147024 grants, respectively. A. Gy. Szanthoffer was supported by the DKOP-23 Doctoral Excellence Program of the Ministry for Culture and Innovation of Hungary from NKFIH. Joanna Jójka acknowledges funding for her doctoral fellowship from the National Science Center, Poland (UMO-2019/32/T/ST8/00265).

Conflicts of Interest

The authors declare no conflict of interest.

References

[1] Valera-Medina A, Amer-Hatem F, Azad AK, Dedoussi IC, et al. Review on ammonia as a potential fuel: From synthesis to economics, Energy Fuels 2021 35:6964–7029. https://doi.org/10.1021/acs.energyfuels.0c03685

[2] Valera-Medina A, Xiao H, Owen-Jones M, David WIF, Bowen PJ. Ammonia for power, Prog Energy Combust Sci 2018 69: 63–102. https://doi.org/10.1016/j.pecs.2018.07.001

[3] Chai WS, Bao Y, Jin P, Tang G, Zhou L. A review on ammonia, ammonia-hydrogen and ammonia-methane fuels, Renew Sustain Energy Rev 2021 147. https://doi.org/10.1016/j.rser.2021.111254

[4] Kobayashi H, Hayakawa A, Somarathne KDKA, Okafor EC. Science and Technology ammonia combustion, Proc Combust Inst 2019 37: 109–133. https://doi.org/10.1016/J.PROCI.2018.09.029

[5] Li J, Lai S, Chen D, Wu R, Kobayashi N, Deng L, Huang H. A Review on Combustion Characteristics of Ammonia as a Carbon-Free Fuel, Front Energy Res 2021 9 https://doi.org/10.3389/fenrg.2021.760356

[6] Cox L. Nitrogen oxides (NOx) why and how they are controlled, Diane Publishing, 1999.

[7] Fritt-Rasmussen J, Gustavson K, Aastrup PJ, Agersted MD, Boertmann D, Clausen DS, Jørgensen CJ, Lansø AS, Mosbech A. Assessment of the potential environmental impacts of a major ammonia spill from a Power-to-X plant and from shipping of ammonia in Greenland, Aarhus University, DCE - Danish Centre for Environment and Energy, 2022. https://pure.au.dk/portal/en/publications/assessment-of-the-potential-environmental-impacts-of-a-major-ammo (Accessed 22 December 2024).

[8] Zhu Y, Curran HJ, Girhe S, Murakami Y, Pitsch H, Senecal K, Yang L, Zhou CW. The combustion chemistry of ammonia and ammonia/hydrogen mixtures: A comprehensive chemical kinetic modeling study, Combust Flame 2024 260 https://doi.org/10.1016/j.combustflame.2023.113239

[9] Han X, Wang Z, Zhou B, He Y, Zhu Y, Cen K, Effect of H2 and O2 enrichment on the laminar burning velocities of NH3+H2+N2+O2 flames: Experimental and kinetic study, Appl Energy Combust Sci 2023 15 https://doi.org/10.1016/j.jaecs.2023.100160

[10] Jian J, Hashemi H, Wu H, Glarborg P, Jasper AW, Klippenstein SJ. An experimental, theoretical, and kinetic modeling study of post-flame oxidation of ammonia, Combust Flame 2024 261 https://doi.org/10.1016/j.combustflame.2024.113325

[11] Otomo J, Koshi M, Mitsumori T, Iwasaki H, Yamada K. Chemical kinetic modeling of ammonia oxidation with improved reaction

mechanism for ammonia/air and ammonia/hydrogen/air combustion, Int J Hydr Energy 2018 43:3004–3014. https://doi.org/10.1016/j.ijhydene.2017.12.066
[12] Stagni A, Arunthanayothin S, Dehue M, Herbinet O, Battin-Leclerc F, Bréquigny P, Mounaïm-Rousselle C, Faravelli T. Low- and intermediate-temperature ammonia/hydrogen oxidation in a flow reactor: Experiments and a wide-range kinetic modeling, Chem Engin J 2023 47, https://doi.org/10.1016/j.cej.2023.144577
[13] Gotama GJ, Hayakawa A, Okafor EC, Kanoshima R, Hayashi M, Kudo T, Kobayashi H. Measurement of the laminar burning velocity and kinetics study of the importance of the hydrogen recovery mechanism of ammonia/hydrogen/air premixed flames, Combust Flame 2022 236 https://doi.org/10.1016/j.combustflame.2021.111753
[14] Liu B, Zhang Z, Yang S, Yu F, Belal BY, Li G. Experimental and chemical kinetic study for the combustion of ammonia-hydrogen mixtures, Fuel 2024 371:131850 https://doi.org/10.1016/j.fuel.2024.131850
[15] Glarborg P. The NH3/NO2/O2 system: Constraining key steps in ammonia ignition and N2O formation, Combust Flame 2023 257 https://doi.org/10.1016/j.combustflame.2022.112311
[16] He X, Li M, Shu B, Fernandes R, Moshammer K. Exploring the Effect of Different Reactivity Promoters on the Oxidation of Ammonia in a Jet-Stirred Reactor, J Phys Chem A 2023 127:1923–1940. https://doi.org/10.1021/acs.jpca.2c07547
[17] Zhang Z, Li A, Li Z, Ren F, Zhu L, Huang Z. An experimental and kinetic modelling study on the oxidation of NH3, NH3/H2, NH3/CH4 in a variable pressure laminar flow reactor at engine-relevant conditions, Combust Flame 2024 265: 113513. https://doi.org/10.1016/j.combustflame.2024.113513
[18] Wang S, Wang Z, Chen C, Elbaz AM, Sun Z, Roberts WL. Applying heat flux method to laminar burning velocity measurements of NH3/CH4/air at elevated pressures and kinetic modeling study, Combust Flame 2022 236 https://doi.org/10.1016/j.combustflame.2021.111788
[19] Meng Q, Lei L, Lee J, Burke MP. On the role of HNNO in NOx formation, Proc Combust Inst 2023 39:551–560. https://doi.org/https://doi.org/10.1016/j.proci.2022.08.044
[20] Klippenstein SJ, Pfeifle M, Jasper AW, Glarborg P. Theory and modeling of relevance to prompt-NO formation at high pressure, Combust Flame 195 (2018) 3–17. https://doi.org/10.1016/j.combustflame.2018.04.029
[21] Glarborg P, Miller JA, Ruscic B, Klippenstein SJ. Modeling nitrogen chemistry in combustion, Prog Energy Combust Sci 2018 67: 31–68. https://doi.org/10.1016/j.pecs.2018.01.002
[22] Mechanical and Aerospace Engineering (Combustion Research), University of California at San Diego, Chemical-Kinetic Mechanisms for Combustion Applications, Https://Web.Eng.Ucsd.Edu/Mae/Groups/Combustion/Mechanism.Html (2018).
[23] Zhang X, Moosakutty SP, Rajan RP, Younes M, Sarathy SM. Combustion chemistry of ammonia/hydrogen mixtures: Jet-stirred reactor measurements and comprehensive kinetic modeling, Combust Flame 2021 234:111653. https://doi.org/10.1016/j.combustflame.2021.111653
[24] Mei B, Zhang J, Shi X, Xi Z, Li Y. Enhancement of ammonia combustion with partial fuel cracking strategy: Laminar flame propagation and kinetic modeling investigation of NH3/H2/N2/air mixtures up to 10 atm, Combust Flame 2021 231:111472. https://doi.org/10.1016/j.combustflame.2021.111472
[25] Marshall P, Glarborg P. Probing High-Temperature Amine Chemistry: Is the Reaction NH3+ NH2⇄ N2H3+ H2 Important?, J Phys Chem A 2023 127 https://doi.org/10.1021/acs.jpca.2c08921
[26] Tamaoki K, Murakami Y, Kanayama K, Tezuka T, Izumi M, Nakamura H. Roles of NH2 reactions in ammonia oxidation at intermediate temperatures: Experiments and chemical kinetic modeling, Combust Flame 2024 259:113177 https://doi.org/10.1016/j.combustflame.2023.113177
[27] Nakamura H, Shindo M. Effects of radiation heat loss on laminar premixed ammonia/air flames, Proc Combust Inst 2019 37:1741–1748. https://doi.org/10.1016/J.PROCI.2018.06.138
[28] Stagni A, Cavallotti C, Arunthanayothin S, Song Y, Herbinet O, Battin-Leclerc F, Faravelli T. An experimental, theoretical and kinetic-modeling study of the gas-phase oxidation of ammonia, React Chem Eng 2020 5 https://doi.org/10.1039/c9re00429g
[29] Miller JA, Bowman CT. Mechanism and modeling of nitrogen chemistry in combustion, Prog Energy Combust Sci 1989 15:287–338. https://doi.org/10.1016/0360-1285(89)90017-8
[30] Klippenstein SJ, Harding LB, Glarborg P, Miller JA. The role of NNH in NO formation and control, Combust Flame 2011 158:774–789.

https://doi.org/10.1016/j.combustflame.2010.12.013
[31] Stagni A, Artioli FR, Frassoldati A, The Role of Radiative Heat Loss and Collisional Energy Transfer in the Flammability Limits of NH3 and NH3–H2 Mixtures, Ind Eng Chem Res 2024 https://doi.org/10.1021/acs.iecr.4c03276
[32] Song Y, Hashemi H, Christensen JM, Zou C, Marshall P, Glarborg P. Ammonia oxidation at high pressure and intermediate temperatures, Fuel 2016 181: 358–365. https://doi.org/10.1016/j.fuel.2016.04.100
[33] Nakamura H, Hasegawa S, Tezuka T. Kinetic modeling of ammonia/air weak flames in a micro flow reactor with a controlled temperature profile, Combust Flame 2017 185: 16–27. https://doi.org/10.1016/j.combustflame.2017.06.021
[34] Kawka L, Juhász G, Papp M, Nagy T, Zsély IG, Turányi T. Comparison of detailed reaction mechanisms for homogeneous ammonia combustion, Zeitschrift Physikalische Chemie 2020 234: 1329–1357. https://doi.org/10.1515/zpch-2020-1649
[35] Szanthoffer AG, Zsély IG, Kawka L, Papp M, Turányi T. Testing of NH_3/H_2 and NH_3/syngas combustion mechanisms using a large amount of experimental data, Appl Energy Combust Sci 2023: 100127. https://doi.org/10.1016/j.jaecs.2023.100127
[36] Girhe S, Snackers A, Lehmann T, Langer R, Loffredo F, Glaznev R, Beeckmann J, Pitsch H. Ammonia and ammonia/hydrogen combustion: Comprehensive quantitative assessment of kinetic models and examination of critical parameters, Combust Flame 2024 267:113560. https://doi.org/10.1016/j.combustflame.2024.113560
[37] Xiao H, Valera-Medina A, Marsh R, Bowen PJ. Numerical study assessing various ammonia/methane reaction models for use under gas turbine conditions, Fuel 2017 196: 344–351 https://doi.org/10.1016/j.fuel.2017.01.095
[38] Duynslaegher C, Contino F, Vandooren J, Jeanmart H. Modeling of ammonia combustion at low pressure, Combust Flame 2012 159: 2799–2805. https://doi.org/10.1016/j.combustflame.2012.06.003
[39] da Rocha RC, Costa M, Bai XS. Chemical kinetic modelling of ammonia/hydrogen/air ignition, premixed flame propagation and NO emission, Fuel 2019 246: 24–33. https://doi.org/10.1016/j.fuel.2019.02.102
[40] Xiao H, Valera-Medina A, Bowen PJ, Dooley S. 3D simulation of ammonia combustion in a lean premixed swirl burner, Energy Procedia 2017 142: 1294–1299.
[41] Nagy T, Turányi T. Reduction of very large reaction mechanisms using methods based on simulation error minimization, Combust Flame 2009 156: 417–428. https://doi.org/10.1016/j.combustflame.2008.11.001
[42] Zsély IG, Nagy T, Simmie JM, Curran HJ. Reduction of a detailed kinetic model for the ignition of methane/propane mixtures at gas turbine conditions using simulation error minimization methods, Combust Flame 2011 158: 1469–1479. https://doi.org/10.1016/j.combustflame.2010.12.011
[43] Valera-Medina A, Giles A, Pugh D, Morris S, Pohl M, Ortwein A. Investigation of combustion of emulated biogas in a gas turbine test rig, J Thermal Science 2018 27: 331–340. https://doi.org/10.1007/s11630-018-1024-1
[44] Chaturvedi S, Santhosh R, Mashruk S, Yadav R, Valera-Medina A. Prediction of NOx emissions and pathways in premixed ammonia-hydrogen-air combustion using CFD-CRN methodology, J Energy Inst 2023 111: 101406. https://doi.org/10.1016/j.joei.2023.101406
[45] Novosselov IV. Chemical Reactor Network Application to Emissions Prediction for Industrial DLE Gas Turbine," Paper No. GT2006-90282, in: ASME International Gas Turbine and Aeroengine Congress. 2006, ASME: Barcelona, Spain, 2006.
[46] Falcitelli M, Pasini S, Rossi N, Tognotti L. CFD+ reactor network analysis: an integrated methodology for the modeling and optimisation of industrial systems for energy saving and pollution reduction, Appl Therm Eng 2002 22: 971–979. https://doi.org/10.1016/S1359-4311(02)00014-5
[47] Fichet V, Kanniche M, Plion P, Gicquel O. A reactor network model for predicting NOx emissions in gas turbines, Fuel 2010 89: 2202–2210. https://doi.org/10.1016/j.fuel.2010.02.010
[48] Mashruk S. NO Formation Analysis using Chemical Reactor Modelling and LIF Measurements on Industrial Swirl Flames, 2020. https://orca.cardiff.ac.uk/id/eprint/136590/ (accessed 22 December 2024).
[49] Frenklach M. Transforming data into knowledge—process informatics for combustion chemistry, Proc Combust Inst 2007 31:125–140. https://doi.org/10.1016/j.proci.2006.08.121
[50] Miller D, Frenklach M. Sensitivity analysis and parameter estimation in dynamic modeling of chemical kinetics, Int J Chem Kinet 1983 15:677–696. https://doi.org/10.1002/kin.550150709
[51] Wang H, Sheen DA. Combustion kinetic model uncertainty quantification, propagation and minimization, Prog Energy Combust Sci 2015 47: 1–31. https://doi.org/10.1016/j.pecs.2014.10.002
[52] Sheen DA, Wang H. The method of uncertainty quantification and minimization using polynomial chaos expansions, Combust Flame 2011 158: 2358–2374. https://doi.org/10.1016/j.combustflame.2011.05.010

[53] Turányi T, Nagy T, Zsély IG, Cserháti M, Varga T, Szabó BT, Sedyó I, Kiss PT, Zempléni A, Curran HJ. Determination of rate parameters based on both direct and indirect measurements, Int J Chem Kinet 2012 44: 284–302. https://doi.org/10.1002/kin.20717
[54] Cai L, Pitsch H. Mechanism optimization based on reaction rate rules, Combust Flame 2014 161: 405–415. https://doi.org/10.1016/j.combustflame.2013.08.024
[55] PrIMe: Process Informatics Model, (2006). primekinetics.org.
[56] Papp M, Varga T, Olm C, Busai A, Nagy T, Zsély IG, Turányi T. ReSpecTh Kinetics Data Format Specification v2.5, 2024.
[57] ReSpecTh information site, 2024.
[58] Papp M, Varga T, Busai A, Zsély IG, Nagy T, Turányi T. Optima++ package v2.5: A general C++ framework for performing combustion simulations and mechanism optimization, 2024. respecth.hu.
[59] Goitom SK, Papp M, Kovács M, Nagy T, Zsély IG, Turányi T, Pál L. Efficient numerical methods for the optimisation of large kinetic reaction mechanisms, Combust Theory Modelling 2022 26: 1071-1097. https://doi.org/10.1080/13647830.2022.2110945
[60] Varga T, Nagy T, Olm C, Zsély IG, Pálvölgyi R, Valkó R, Vincze G, Cserháti M, Curran HJ, Turányi T. Optimization of a hydrogen combustion mechanism using both direct and indirect measurements, Proc Combust Inst 2015 35: 589–596. https://doi.org/10.1016/j.proci.2014.06.071
[61] Kovács M, Papp M, Zsély IG, Turányi T. Determination of rate parameters of key N/H/O elementary reactions based on H2/O2/NOx combustion experiments, Fuel 2020 264: 116720. https://doi.org/https://doi.org/10.1016/j.fuel.2019.116720
[62] Nagy T, Turányi T. Uncertainty of Arrhenius parameters, Int J Chem Kinet 2011 43: 359–378. https://doi.org/10.1002/kin.20551
[63] Nagy T, Valkó E, Sedyó I, Zsély IG, Pilling MJ, Turányi T. Uncertainty of the rate parameters of several important elementary reactions of the H_2 and syngas combustion systems, Combust Flame 2015 162: 2059–2076. https://doi.org/10.1016/j.combustflame.2015.01.005
[64] Saltelli A, Tarantola S, Campolongo F, Ratto M. Sensitivity Analysis in Practice. A Guide to Assessing Scientific Models. In: Probability and Statistics Series., Wiley, 2004.
[65] Kovács M, Papp M, Turányi T, Nagy T. A novel active parameter selection strategy for the efficient optimization of combustion mechanisms, Proc Combust Inst 2023 39: 5259–5267. https://doi.org/10.1016/j.proci.2022.07.241
[66] Jasper AW. Predicting third-body collision efficiencies for water and other polyatomic baths, Faraday Discuss 2022 238: 68–86. https://doi.org/10.1039/D2FD00038E
[67] Glarborg P, Hashemi H, Cheskis S, Jasper AW. On the rate constant for NH2+HO2and third-body collision efficiencies for NH2+H(+M) and NH2+NH2(+M), J Phys Chem A 2021 125: 1505–1516. https://doi.org/10.1021/acs.jpca.0c11011
[68] Sabia P, Manna MV, Ragucci R, de Joannon M. Mutual inhibition effect of hydrogen and ammonia in oxidation processes and the role of ammonia as “strong” collider in third-molecular reactions, Int J Hydrogen Energy 2020 45: 32113–32127. https://doi.org/10.1016/j.ijhydene.2020.08.218
[69] Hayakawa A, Hayashi M, Kovaleva M, Gotama GJ, Okafor EC, Colson S, Mashruk S, Valera-Medina A, Kudo T, Kobayashi H. Experimental and numerical study of product gas and N2O emission characteristics of ammonia/hydrogen/air premixed laminar flames stabilized in a stagnation flow, Proc Combust Inst 2023 39: 1625–1633. https://doi.org/10.1016/j.proci.2022.08.124
[70] Szanthoffer AG, Papp M, Turányi T. Identification of well-parameterised reaction steps in detailed combustion mechanisms – A case study of ammonia/air flames, Fuel 2025 380: 132938. https://doi.org/10.1016/j.fuel.2024.132938
[71] Osipova KN, Zhang X, Sarathy SM, Korobeinichev OP, Shmakov AG. Ammonia and ammonia/hydrogen blends oxidation in a jet-stirred reactor: Experimental and numerical study, Fuel 2022 310: 122202. https://doi.org/https://doi.org/10.1016/j.fuel.2021.122202
[72] Karan A, Dayma G, Chauveau C, Halter F. Experimental study and numerical validation of oxy-ammonia combustion at elevated temperatures and pressures, Combust Flame 2022 236 https://doi.org/10.1016/j.combustflame.2021.111819
[73] Nagy T, Turányi T. Minimal Spline Fit: a model-free method for determining statistical noise of experimental data series, Proc European Combust Meeting, Paper 336, 2021.
[74] Olm C, Varga T, Valkó E, Curran HJ, Turányi T. Uncertainty quantification of a newly optimized methanol and formaldehyde combustion mechanism, Combust Flame 2017 186: 45–64. https://doi.org/10.1016/j.combustflame.2017.07.029
[75] Lee JH, Kim JH, Park JH, Kwon OC. Studies on properties of laminar premixed hydrogen-added ammonia/air flames for hydrogen production, Int J Hydrogen Energy 2010 35: 1054–1064. https://doi.org/10.1016/j.ijhydene.2009.11.071
[76] Lee JH, Lee SI, Kwon OC. Effects of ammonia substitution on hydrogen/air flame propagation and emissions, Int J Hydrogen Energy 2010 35: 11332–

11341. https://doi.org/10.1016/j.ijhydene.2010.07.104
[77] Hayakawa A, Goto T, Mimoto R, Arakawa Y, Kudo T, Kobayashi H. Laminar burning velocity and Markstein length of ammonia/air premixed flames at various pressures, Fuel 2015 159: 98–106. https://doi.org/10.1016/j.fuel.2015.06.070
[78] Ichikawa A, Hayakawa A, Kitagawa Y, Somarathne KDKA, Kudo T, Kobayashi H. Laminar burning velocity and Markstein length of ammonia/hydrogen/air premixed flames at elevated pressures, Int J Hydrogen Energy 2015 40: 9570–9578. https://doi.org/10.1016/j.ijhydene.2015.04.024
[79] Li Y, Bi M, Li B, Gao W. Explosion behaviors of ammonia–air mixtures, Combust Sci Tech 2018 190: 1804–1816. https://doi.org/10.1080/00102202.2018.1473859
[80] Han X, Wang Z, Costa M, Sun Z, He Y, Cen K. Experimental and kinetic modeling study of laminar burning velocities of NH3/air, NH3/H2/air, NH3/CO/air and NH3/CH4/air premixed flames, Combust Flame 2019 206: 214–226. https://doi.org/10.1016/j.combustflame.2019.05.003
[81] Liu Q, Chen X, Huang J, Shen Y, Zhang Y, Liu Z. The characteristics of flame propagation in ammonia/oxygen mixtures, J Hazard Mater 2019 363: 187–196. https://doi.org/https://doi.org/10.1016/j.jhazmat.2018.09.073
[82] Mei B, Zhang X, Ma S, Cui M, Guo H, Cao Z, Li Y. Experimental and kinetic modeling investigation on the laminar flame propagation of ammonia under oxygen enrichment and elevated pressure conditions, Combust Flame 2019 210: 236–246. https://doi.org/10.1016/j.combustflame.2019.08.033
[83] Han X, Wang Z, He Y, Liu Y, Zhu Y, Konnov AA. The temperature dependence of the laminar burning velocity and superadiabatic flame temperature phenomenon for NH3/air flames, Combust Flame 2020 217: 314–320. https://doi.org/10.1016/j.combustflame.2020.04.013
[84] Lesmana H, Zhu M, Zhang Z, Gao J, Wu J, Zhang D. Experimental and kinetic modelling studies of laminar flame speed in mixtures of partially dissociated NH3 in air, Fuel 2020 278: 118428. https://doi.org/10.1016/j.fuel.2020.118428
[85] Lhuillier C, Brequigny P, Lamoureux N, Contino F, Mounaïm-Rousselle C. Experimental investigation on laminar burning velocities of ammonia/hydrogen/air mixtures at elevated temperatures, Fuel 2020 263 https://doi.org/10.1016/j.fuel.2019.116653
[86] Wang S, Wang Z, Elbaz AM, Han X, He Y, Costa M, Konnov AA, Roberts WL. Experimental study and kinetic analysis of the laminar burning velocity of NH3/syngas/air, NH3/CO/air and NH3/H2/air premixed flames at elevated pressures, Combust Flame 2020 221: 270–287. https://doi.org/10.1016/j.combustflame.2020.08.004
[87] Wang D, Ji C, Wang Z, Wang S, Zhang T, Yang J. Measurement of oxy-ammonia laminar burning velocity at normal and elevated temperatures, Fuel 2020 279: 118425. https://doi.org/10.1016/j.fuel.2020.118425
[88] Xia Y, Hashimoto G, Hadi K, Hashimoto N, Hayakawa A, Kobayashi H, Fujita O. Turbulent burning velocity of ammonia/oxygen/nitrogen premixed flame in O2-enriched air condition, Fuel 2020 268: 117383. https://doi.org/https://doi.org/10.1016/j.fuel.2020.117383
[89] Kim HK, Ku JW, Ahn YJ, Kim YH, Kwon OC. Effects of O2 enrichment on NH3/air flame propagation and emissions, Int J Hydrogen Energy 2021 46: 23916–23926. https://doi.org/10.1016/j.ijhydene.2021.04.154
[90] Li Y, Bi M, Zhang K, Gao W. Effects of nitrogen and argon on ammonia-oxygen explosion, Int J Hydrogen Energy 2021 46: 21249–21259. https://doi.org/10.1016/j.ijhydene.2021.03.212
[91] Osipova KN, Korobeinichev OP, Shmakov AG. Chemical structure and laminar burning velocity of atmospheric pressure premixed ammonia/hydrogen flames, Int J Hydrogen Energy 2021 46: 39942–39954. https://doi.org/https://doi.org/10.1016/j.ijhydene.2021.09.188
[92] Shrestha KP, Lhuillier C, Barbosa AA , Brequigny P, Contino F, Mounaïm-Rousselle C, Seidel L, Mauss F. An experimental and modeling study of ammonia with enriched oxygen content and ammonia/hydrogen laminar flame speed at elevated pressure and temperature, Proc Combust Inst 2021 38: 2163–2174. https://doi.org/10.1016/j.proci.2020.06.197
[93] Wang N, Huang S, Zhang Z, Li T, Yi P, Wu D, Chen G. Laminar burning characteristics of ammonia/hydrogen/air mixtures with laser ignition, Int J Hydrogen Energy 2021 46: 31879–31893. https://doi.org/https://doi.org/10.1016/j.ijhydene.2021.07.063
[94] Han X, Wang Z, He Y, Zhu Y, Lin R, Konnov AA. Uniqueness and similarity in flame propagation of pre-dissociated NH3 + air and NH3 + H2 + air mixtures: An experimental and modelling study, Fuel 2022 327: 125159. https://doi.org/10.1016/j.fuel.2022.125159
[95] Hou D, Zhang Z, Cheng Q, Liu B, M Zhou, Li G. Experimental and kinetic studies of laminar burning velocities of ammonia with high Lewis number at elevated pressures, Fuel 2022 320: 123913. https://doi.org/10.1016/j.fuel.2022.123913
[96] Ji C, Wang Z, Wang D, Hou R, Zhang T, Wang S. Experimental and numerical study on premixed

partially dissociated ammonia mixtures. Part I: Laminar burning velocity of NH3/H2/N2/air mixtures, Int J Hydrogen Energy 2022 47: 4171–4184. https://doi.org/https://doi.org/10.1016/j.ijhydene.2021.10.269

[97] Zitouni S, Brequigny P, Mounaïm-Rousselle C. Influence of hydrogen and methane addition in laminar ammonia premixed flame on burning velocity, Lewis number and Markstein length, Combust Flame 2023 253: 112786. https://doi.org/10.1016/J.COMBUSTFLAME.2023.112786

[98] Goodwin DG, Moffat HK, Schoegl I, Speth RL, Weber BW. Cantera: An Object-oriented Software Toolkit for Chemical Kinetics, Thermodynamics, and Transport Processes, (2022). https://doi.org/10.5281/ZENODO.6387882

[99] Mashruk S, Alnasif A, Yu C, Thatcher J, Rudman J, Peronski L, Meng-Choung C, Valera-Medina A. Combustion Characteristics of a Novel Ammonia Combustor equipped with Stratified Injection for Low Emissions, J Ammonia Energy 2023 1: 21-32. https://doi.org/10.18573/JAE.10

[100] ANSYS Inc., Ansys Fluent Theory Guide, Canonsburg, 2024. http://www.ansys.com

[101] Alnasif A, Mashruk S, Shi H, Alnajideen M, Wang P, Pugh D, Valera Medina A. Evolution of ammonia reaction mechanisms and modeling parameters: A review, Appl Energy Combust Sci 2023 15: 100175. https://doi.org/10.1016/j.jaecs.2023.100175

[102] Alnasif A, Jójka J, Mashruk S, Nagy T, Valera-Medina A. Analysis of the performance of kinetic reaction mechanisms in estimating N2O mole fractions in 70/30 vol% NH3/H2 premixed flames, Fuel 2024 371: 131897. https://doi.org/10.1016/j.fuel.2024.131897

[103] Alnasif A, Mashruk S, Hayashi M, Jójka J, Shi H, Hayakawa A, Valera-Medina A. Performance Investigation of Currently Available Reaction Mechanisms in the Estimation of NO Measurements: A Comparative Study, Energies 2023 6: 3847 https://doi.org/10.3390/EN16093847

[104] Mashruk S, Zitouni SE, Brequigny P, Mounaim-Rousselle C, Valera-Medina A. Combustion performances of premixed ammonia/hydrogen/air laminar and swirling flames for a wide range of equivalence ratios, Int J Hydr Energy 2022 47: 41170–41182. https://doi.org/10.1016/j.ijhydene.2022.09.165

[105] Lamoureux N, Desgroux P, El Bakali A, Pauwels JF. Experimental and numerical study of the role of NCN in prompt-NO formation in low-pressure CH4-O2-N2 and C2H2-O2-N2 flames, Combust Flame 2010 157: 1929–1941. https://doi.org/10.1016/j.combustflame.2010.03.013

[106] Han X, Lavadera L, Konnov AA. An experimental and kinetic modeling study on the laminar burning velocity of NH3+N2O+air flames, Combust Flame 2021 228: 13–28. https://doi.org/10.1016/j.combustflame.2021.01.027

[107] Alnasif A, Mashruk S, Jójka J, Nagy T, Valera-Medina A. Comprehensive investigation of available reaction mechanisms in their performance of estimation of NO2 concentration in 70/30 vol% NH3/H2 Premixed Flames, Presented at: Cardiff Engineering Research Conference, 12-14 July 2023. https://orca.cardiff.ac.uk/id/eprint/161458/ (accessed 22 December 2024).

[108] Alnasif A, Jójka J, Mashruk S, Davies J, Nagy T, Valera-Medina A. A kinetic modelling study for estimating residual NH3 speciation at the combustion outlet in 70/30 vol% NH3/H2 flames, Presented at: 2nd Symposium on Ammonia Energy, 11-13 July 2023. https://orca.cardiff.ac.uk/id/eprint/161456

[109] Innocenti A, Andreini A, Bertini D, Facchini B, Motta M. Turbulent flow-field effects in a hybrid CFD-CRN model for the prediction of NOx and CO emissions in aero-engine combustors, Fuel 2018 215: 853–864. https://doi.org/https://doi.org/10.1016/j.fuel.2017.11.097

[110] Savarese M, Giuntini L, Malpica Galassi R, Iavarone S, Galletti C, De Paepe W, Parente A. Model-to-model Bayesian calibration of a Chemical Reactor Network for pollutant emission predictions of an ammonia-fuelled multistage combustor, Int J Hydr Energy 2024 49: 586–601. https://doi.org/https://doi.org/10.1016/j.ijhydene.2023.08.275